IIETA International Information and Engineering Technology Association
Advancing the World of Information and Engineering

Annales de Chimie - Science des Matériaux
Vol. 48, No. 5, October, 2024, pp. 729-737
Journal homepage: http://iieta.org/journals/acsm

Molecular Dynamics Simulation to Predict Virgin Bitumen Structural Properties

Khadidja Rouidi[1*], Habib Trouzine[1,2], Asroun Aissa[1], Bezzar Abdelillah[2,3]

[1] Civil Engineering and Environmental Laboratory, Faculty of Technology, Sidi Bel Abbes University, Sidi Bel Abbes 22000, Algeria
[2] Civil Engineering Department, Tlemcen University, Tlemcen 13000, Algeria
[3] Faculty of Technology, Tlemcen University, Tlemcen 13000, Algeria

Corresponding Author Email: rouidi-khadidja@hotmail.fr

https://doi.org/10.18280/acsm.480514

Received: 15 August 2024
Revised: 9 October 2024
Accepted: 18 October 2024
Available online: 29 October 2024

Keywords:
bitumen, MDS, mechanical properties, Young's modulus, temperature

ABSTRACT

Bitumen, which is crucial to road and asphalt construction, significantly impacts the long-term viability and performance of transportation infrastructure. Understanding bitumen's intricate molecular composition and behavior is crucial to improving its properties and developing practical materials and methods. Molecular dynamics simulations (MDS) have recently become popular as a powerful method of molecular-level study of bitumen. The article's study describes MD simulations' applications and advanced features regarding three types of bitumen: AAA-1, AAK-1, and AAM-1. It discusses the interactions between molecules, the behavior of phases, the mechanical properties of bitumen, and the effects of temperature. The review's conclusion states that the potential of MDS to facilitate further advances in the study of bitumen is evident; this will lead to an enhanced understanding of the material and improved bitumen products and infrastructure.

1. INTRODUCTION

Bitumen, also known as asphalt, remains a fundamental material in the construction industry, particularly for road pavements, due to its excellent mechanical properties and cost-effectiveness [1-3]. The mechanical behavior of bitumen is crucial in determining the overall performance and durability of asphalt pavements under various loading and environmental conditions [4]. Recent advancements in research have shed light on understanding the intricate mechanical properties of bitumen using both experimental and computational approaches [5-8].

Over the years, MDS has become a valuable tool in predicting the mechanical characteristics of materials on a molecular scale. By employing computer algorithms and mathematical models, this approach simulates the behavior of atoms and molecules, offering insights into the dynamic properties of various materials. In bitumen research, MDS has demonstrated its potency in forecasting the properties of asphalt compositions [9-14].

In bitumen research, MDS has demonstrated its efficiency in predicting the mechanical properties of different bitumen combinations [13, 15-17]. The purpose of this article is to explore the mechanical properties of three kinds of bitumen material SARA fractions (Saturate, Asphaltene, Resin, and Aromatic): AAA-1, AAK-1, and AAM-1 [13, 18-21] at different temperatures using MDS.

The LAMMPS (Large-Scale Atomic/Molecular Massively Parallel Simulator) software will be used to accurately simulate the behavior of bitumen molecules [22, 23]. To ensure the reliability and legitimacy of the simulation results, the PCFF (Polymer Consistent Force Field) class II will be employed [24-26]. This field of force is commonly utilized in the research field of bitumen [27, 28] because it accurately describes the interactions between molecules and reproduces experimental results. Using the PCFF field of force, we can produce accurate and legitimate predictions of the mechanical properties of bitumen.

In this study, MDS is employed to estimate viscosity and investigate the behavior of the Young's modulus with varying temperatures (223.15 K, 248.15 K, 273.15 K, 298.15 K, 323.15 K, and 348.15 K) for three distinct bitumen materials: AAA-1, AAK-1, and AAM-1, this spectrum of temperature encompasses standard room temperature through typical paving operation temperatures.

2. MATERIAL AND METHODS

2.1 Bitumen

The original asphalt samples used in this study are AAA-1, AAK-1 and AAM-1 commonly used in scientific research. These special bitumen samples typically come from the following regions: Canada, Venezuela, and the USA. The elemental analysis of SHRP core bitumen is shown in Table 1.

Bitumen samples from different geographical locations have different chemical compositions, which affects their physical and rheological properties [29, 30]. Elemental analysis provides important insights into the fundamental

molecular structure and heterogeneity of these asphalt materials. Table 1 provides a comprehensive overview of the elemental composition, including the relative abundance of carbon, hydrogen, nitrogen, sulfur, and other trace elements in the SHRP bitumen core samples examined.

Table 1. Elemental analysis for the core SHRP bitumens [31]

Origin	Unit	AAA-1	AAK-1	AAM-1
		Canada	Venezuela	USA
C	wt.%	83.9	83.7	86.8
H	wt.%	10.0	10.2	11.2
H+C	wt.%	93.9	93.9	98.0
H/C	Molar	1.43	1.46	1.55
O	wt.%	0.6	0.8	0.5
N	wt.%	0.5	0.7	0.6
S	wt.%	5.5	6.4	1.2
V	ppm	174	1480	58
Ni	ppm	86	142	36
Mn	g/mol	790	860	1300

By characterizing the elemental composition, researchers can establish correlations between chemical composition and observed asphalt performance characteristics. This information can serve as a basis for further studies on molecular structure, aging behavior and possible modifications to improve the durability and functionality of asphalt materials in various applications such as roads and road construction. Table 2 described the typical values for penetration at 25℃ for AAA-1, AAK-1 and AAM-1 bitumens according to Laux et al. [30].

Table 2. Typical values for penetration at 25℃ for AAA-1, AAK-1 and AAM-1 [31]

Bitumen Origin	Bitumen Name	Penetration at 25℃
Lloydminster	AAA-1	155
Boscan	AAK-1	65
West Texas Intermediate	AAM-1	63

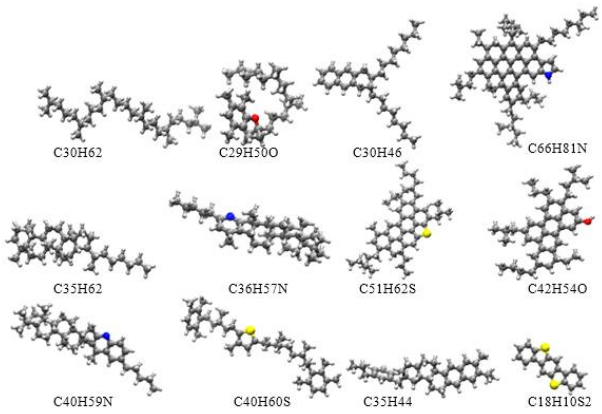

Figure 1. Molecular models of bitumen [32]

2.2 Molecular model of bitumen

Bitumen has four distinct components: saturate, aromatic, resin and asphaltene SARA fractions. Given the intricate nature of these components, selecting an appropriate molecular model is crucial to improve the precision of molecular simulations. For this study, the 12-molecule bitumen model, as illustrated in Figure 1, was utilized to represent bitumen, thus, its three kinds were detailed as shown in Table 3 [32].

Table 3. Chemical characteristics of three kinds of bitumen AAA-1 AAK-1 and AAM-1 [32]

SARA Fractions	Molecule	Number of molecules in model system			Molar Mass
		AAA-1	AAK-1	AAM-1	
Saturate	C30H62	4	2	1	422.9
	C35H62	4	2	1	483.0
Aromatic	C30H46	13	10	21	406.8
	C35H44	11	10	20	464.8
Resin	C29H50O	5	4	10	414.8
	C36H57N	4	4	10	530.9
	C18H10S2	15	12	4	290.4
	C40H60S	4	4	10	554.0
	C40H59N	4	4	10	573.1
Asphaltene	C66H81N	2	2	1	888.5
	C51H62S	3	3	1	707.2
	C42H54O	3	3	1	575.0

The approach developed by Li and Greenfield [32] has been effectively utilized in various studies on nanoscale asphalt, highlighting the significance of a robust molecular model for asphalt binders in understanding its performance at the molecular level.

The 12-molecule model strikes an effective balance between computational efficiency and precision, allowing extended simulation periods and repeated trials while demanding fewer computational resources than larger alternatives. Rooted in the well-established SHRP (Strategic Highway Research Program) framework, this model has been validated through extensive research and experimental studies, ensuring its reliability in evaluating essential properties of bitumen.

Moreover, it encompasses crucial molecular groups in real bitumen, such as saturates, aromatics, resins, and asphaltenes, thus preserving a realistic distribution of molecular weights. Compared to more intricate models, it offers quicker equilibration times, simplifies the examination of molecular interactions, and is ideal for exploring fundamental characteristics and conducting comparative analyses.

2.3 PCFF force field parameters

Polymer Consistent Force Field (PCFF) has been utilized in our simulation to estimate the properties of bitumen systems. In essence, PCFF is a class II force field that aims to describe non-bonded van der Waals and electrostatic interactions between atoms; total potential energy comprises valence and non-bond terms, as detailed in Eq. (1).

$$E_{total} = \sum E^b + \sum E^a + \sum E^t + \sum E^o + \sum E^{bb'} + \sum E^{ba} + \sum E^{bt} + \sum E^{aa'} + \sum E^{at} + \sum E^{aa't} + \sum E^{vdw} + \sum E^{elec} \quad (1)$$

where, E^b, E^a, E^t, E^o, $E^{bb'}$, E^{ba}, E^{bt}, $E^{aa'}$, E^{at}, $E^{aa't}$ are Valence terms, and E^{vdw} and E_{elec} are Non-bond terms.

E^b, E^a, E^t, E^o are bond energy, angle energy, torsion angle energy, and out-of-plane angle energy, respectively. The interconnection between them is $E^{bb'}$, E^{ba}, E^{bt}, $E^{aa'}$, E^{at}, $E^{aa't}$.

E^{vdw} Van der Waals energy illustrated by Lennard-Jones

(LJ) 9-6 potential in Eq. (2).

$$E^{vdw} = \varepsilon_{ij}\left[2\left(\frac{r_{ij}^0}{r_{ij}}\right)^9 - 3\left(\frac{r_{ij}^0}{r_{ij}}\right)^6\right] \quad (2)$$

E^{elec} Coulombic electrostatic energy illustrated Coulombic forces in Eq. (3).

$$E^{elec} = \frac{q_i\, q_j}{r_{ij}} \quad (3)$$

where,

ε_{ij} is the well depth.

r_{ij}^0 is the distance at which the LJ potential is zero.

r_{ij} is the interatomic distance i and j, respectively.

q_i, q_j are partial charges.

2.4 Young's modulus

Young's modulus is a fundamental material property that plays a crucial role in determining the strain response of a material under applied loads and the deformation behavior of a structure. Accurate determination of this parameter is critical for engineers to perform reliable computer simulations and accurately predict structural response. As an important input to computational models, the elastic modulus accurately predicts the stress distribution, deformation and overall mechanical properties of technical systems under different loading conditions [33].

While Young's modulus is not directly calculated in MDS, certain analytical methods can be employed to estimate it. Young's modulus is a metric that gauges the rigidity of a substance and illustrates how it reacts to applied stress.

The Stress-Strain Method involves applying strain to the system and measuring the resultant stress. The slope of the stress-strain curve in the elastic region can be used to approximate the value of Young's modulus Eq. (4).

$$E = \frac{stress}{strain} = \frac{\sigma}{\varepsilon} \quad (4)$$

where,

E = Young's modulus (GPa);

σ = stress (GPa);

ε = strain.

3. MOLECULAR DYNAMICS (MD) SIMULATIONS RESULTS AND DISCUSSION

3.1 Construction and equilibration of bitumen model

For all simulations conducted in this study, the LAMMPS software was utilized. The chosen model for bitumen was the classical 12- model. The proposed component model by Laux et al. [30] is focused on classifying bitumen into three distinct types. These types are identified as AAA-1, AAK-1, and AAM-1.

To create the amorphous cell module, twelve individual components were combined into a cubic shape with an initial density of 0.1 g/cm^3 at a temperature of 298.15 K and a cutoff of 12.5Å using 1 fs time steps for 500000 steps to manage potential early-stage force interactions.

The entirety of the structure was relaxed through a 5000 step geometry optimization process with conjugate gradient.

A dynamic simulation NVT was conducted for 500 ps to stabilize the model. Afterward, a dynamic simulation in NPT was executed at 298.15 K and 1 atm for duration of 500 ps, Figure 2 illustrates equilibration of AAK-1 as an example.

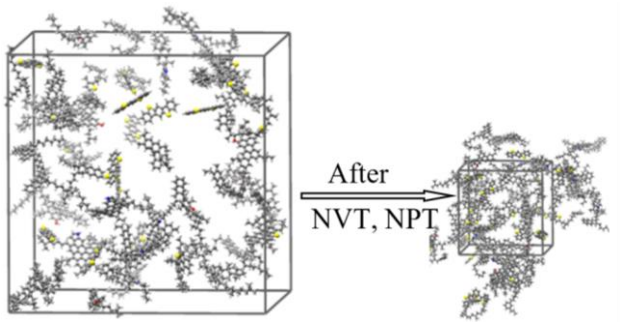

Figure 2. Molecular model of bitumen AAK-1 before and after equilibration

The ultimate densities of AAA-1, AAK-1, and AAM-1 were recorded as 0.947 g/cm^3, 0.965 g/cm^3, 0.936 g/cm^3, respectively, as illustrated in Figure 3.

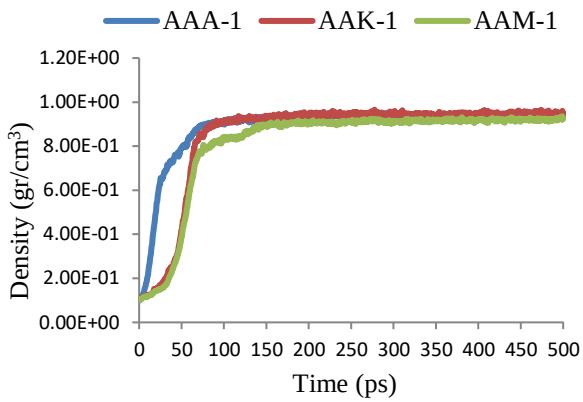

Figure 3. Density curve of three types of bitumen AAA-1, AAK-1, and AAM-1

3.2 Models validation

We calculated densities, cohesive energy densities, solubility and glass transition to support our research findings. These values were then compared to the results of molecular dynamics calculations and experimental studies. The contrasting analysis is listed in Table 4.

The measure of cohesive energy density CED Eq. (5) determines the level of cohesion within a substance.

$$CED = \frac{E_{coh}}{V} \quad (5)$$

The assessment of intermolecular interaction within a bitumen molecule model is determined through the mutual attraction of molecules, which can be used to define a solubility parameter that can be calculated from the CED using Eq. (6).

$$\delta = \sqrt{\text{CED}} \quad (6)$$

Table 4. Calculated Properties of three types of bitumen AAA-1 AAK-1 AAM-1 with MD Simulation

Parameters	AAA-1	AAK-1	AAM-1	References
Density (gr/cm^3) (298.15 K)	0.947	0.965	0.936	[15, 34-38]
CED (10^8 J/m^3)	3.05	3.21	2.07	[39-41]
δ ($(J/cm^3)^{1/2}$)	17.46	17.92	14.4	[32, 38, 40-41]
Tg (K)	251.48	250.82	249.61	[15, 20, 34, 42]
Viscosity (cP) (298.15 K)	1.41	1.95	1.60	[43-46]

The point at which the mechanical states of asphalt shift from a viscoelastic state to a glassy state is called the Tg, or glass transition temperature, as illustrated in Figure 4.

The viscosity [47, 48] of bitumen MD models was calculated by Green Kubo formula. The code which is based on LAMMPS documentation. The simulations were conducted under NVT ensemble for 10 ns and at a temperature of 298.15 K.

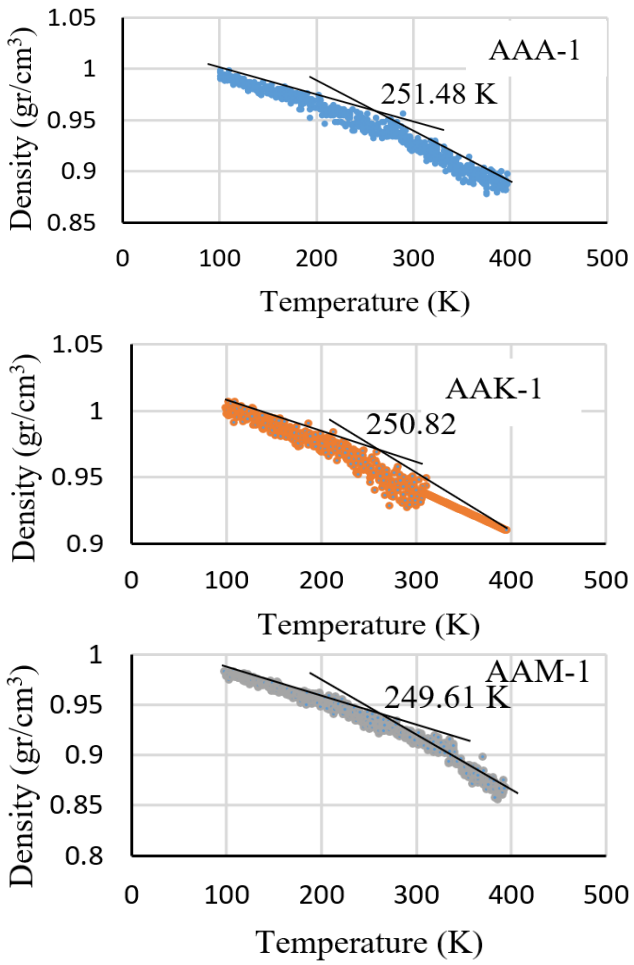

Figure 4. Glass transition curve of three types of bitumen AAA-1, AAK-1, and AAM-1

3.3 Young's Modulus of three bitumen models

Following the equilibration of the three types of bitumen, a molecular dynamics (MD) tensile simulation is conducted throughout 20 ps. The simulation involves subjecting the NPT ensemble to a total deformation along the x-axis at a temperature of 298.15 K. Subsequently; the stress-strain outcomes were collected every 175 fs and visually depicted in Figure 5.

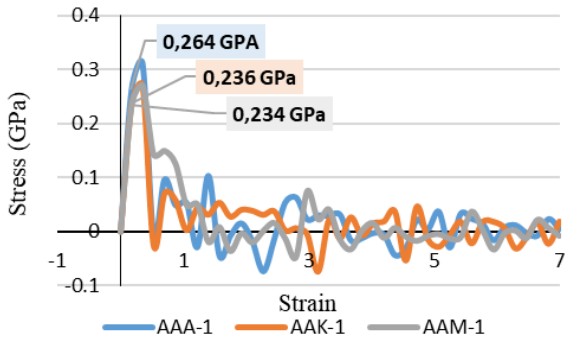

Figure 5. Stress-Strain curve of three types of bitumen AAA-1, AAK-1, and AAM-1 at 298.15 K

The values indicated on the curves signify the end of elastic limit. By calculating the slope of each straight line within the elastic region of the three curves, the Young's modulus values of AAA-1, AAK-1, and AAM-1 were determined to be E = 1.506 GPa, E = 1.348 GPa, and E = 1.337 GPa, respectively. Based on the MDS and experimental provided references, these values fall within the range of 1 GPa to 2 GPa [15, 49, 50].

To investigate the impact of temperature on the tensile simulation outcomes for the AAA-1, AAK-1, and AAM-1 bitumen models, a range of five temperatures (-75 ℃ (223.15 K), -25 ℃ (248.15 K), 0 ℃ (273.15 K), 50 ℃ (323.15 K), and 75 ℃ (348.15 K)) were chosen. These selected temperatures enable the examination and analysis of the tensile properties of the three bitumen models across a spectrum from extremely low to exceedingly high temperatures. The results are illustrated in Figures 6-8.

In line with the previous section, the Young's modulus values of each type of bitumen AAA-1, AAK-1, and AAM-1, at various temperatures, are listed in the following Table 5.

It's observed that as the temperature increased, the Young's modulus decreased for all three materials. This conforms to theoretical predictions [51, 52], where thermal energy weakens intermolecular bonds and makes materials more easily deformed when heated.

Across the temperatures examined, AAA-1 was identified as having the greatest Young's modulus, hinting at its elastic rigidity enduring the interference of thermal energy on molecular structure with a rigidity loss on the order of 381 MPa between 223.15 K and 348.15 K. Conversely, AAK-1 and AAM-1 each had visibly lower Young's modulus with a rigidity loss of 557 MPa and 406 MPa respectively; possibly suggesting their structures were more susceptible to deformation with elevated temperatures.

Table 5. Young's Modulus value of three types of bitumen AAA-1 AAK-1 AAM-1 under different temperatures

Temperature (K)	E (GPa)		
	AAA-1	AAK-1	AAM-1
223.015	1.790	1.737	1.669
248.15	1.662	1.569	1.556
273.15	1.579	1.440	1.454
298.15	1.506	1.348	1.337
323.15	1.496	1.290	1.277
348.15	1.409	1.180	1.263

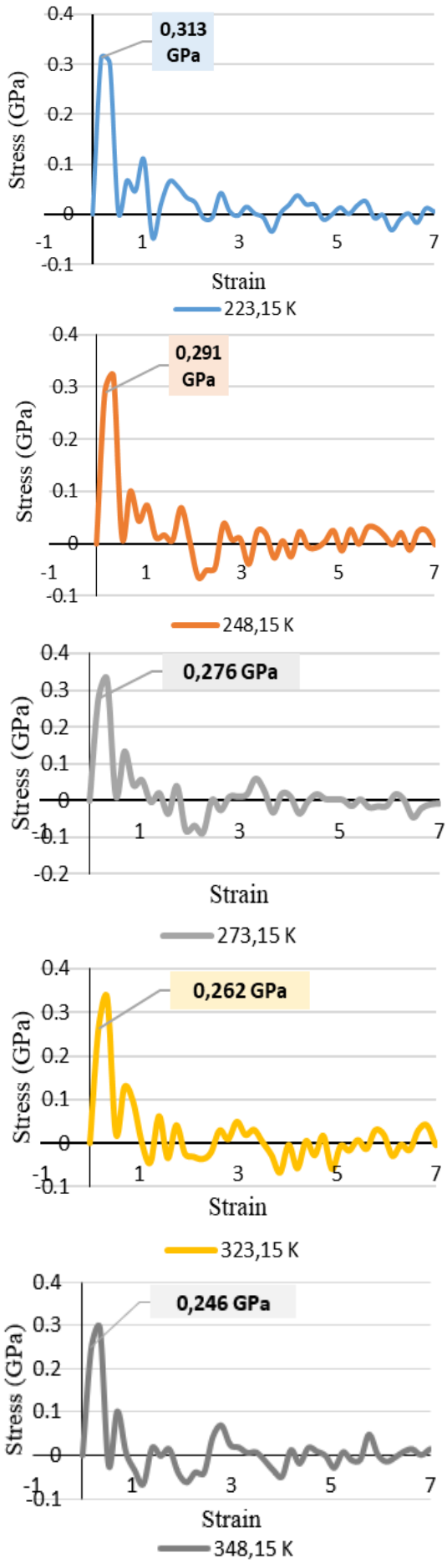

Figure 6. Stress-Strain curves of AAA-1 bitumen under 223.15 K, 248.15 K, 273.15 K, 323.15 K and 348.15 K

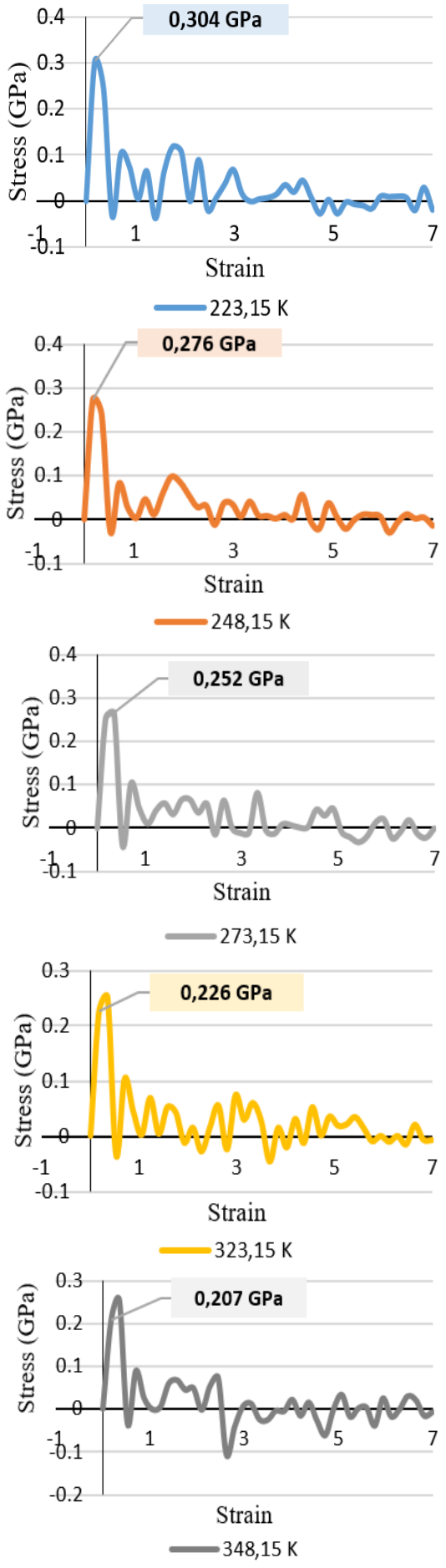

Figure 7. Stress-Strain curves of AAK-1 bitumen under 223.15 K, 248.15 K, 273.15 K, 323.15 K and 348.15 K

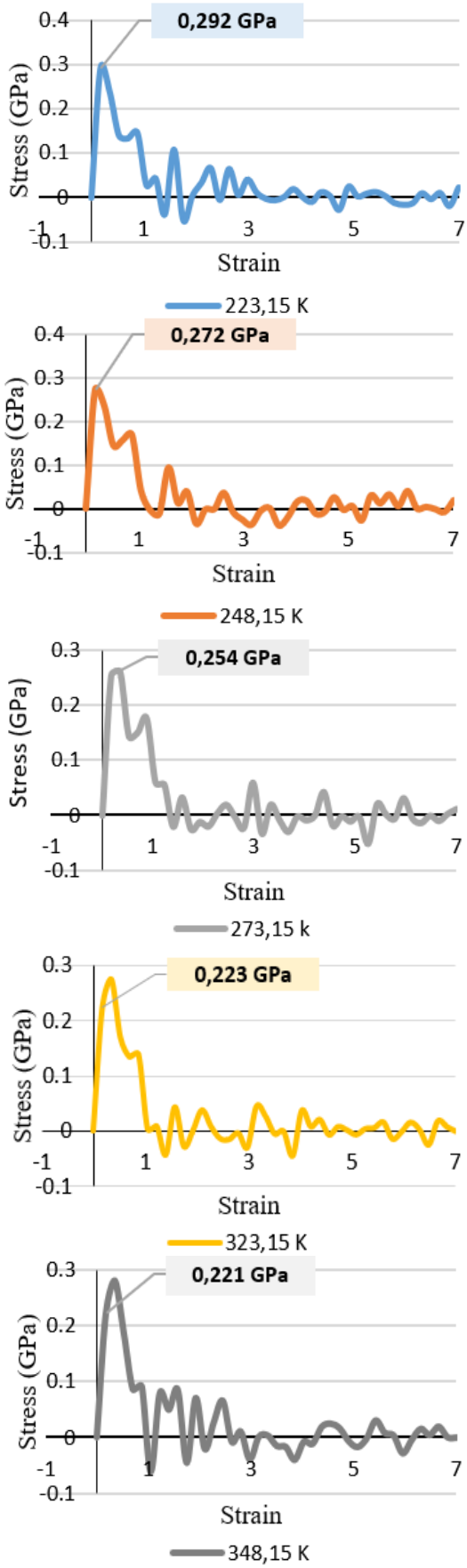

Figure 8. Stress-Strain curves of AAM-1 bitumen under 223.15 K, 248.15 K, 273.15 K, 323.15 K and 348.15 K

To support these results and analyze them effectively, a (MDS) was conducted for the three types of bitumen, AAA-1, AAK-1, and AAM-1, at room temperature (298.15 K) along the y and z-axis. Young's modulus results of the three types of bitumen are illustrated in Table 6.

Table 6. Young's Modulus value of three types of bitumen AAA-1, AAK-1, AAM-1 at 298.15 K along y and z axis

Axis	E (GPa)		
	AAA-1	AAK-1	AAM-1
y	1.099	1.333	1.305
z	2.218	1.194	1.235

The outcomes of the molecular dynamics calculations showed different variations in Young's modulus for the different types of bitumen and the different loading directions. In the x-axis direction, AAA-1 demonstrated the greatest Young's modulus, followed by AAK-1 and AAM-1. This trend is attributed to specific molecular associations and chemical forces between molecules within each composition, these forces influence the mechanical behavior of the composition.

In the y-axis direction, AAK-1 demonstrated the greatest Young's modulus with 1.333 GPa, indicating its increased tensile strength compared to AAA-1 and AAM-1, with values of Young's modulus 1.099 GPa and 1.305 GPa, respectively. The molecular composition of AAK-1 may have a role in the increased strength of the intermolecular interactions and the more effective transmission of loads in this direction. The Young's modulus of the y-axis was lower for the AAA-1 and AAM-1, which suggests that they have a decreased resistance to deformation.

In the z-axis direction, AAA-1 exhibited once again the greatest Young's modulus with 2.218 GPa, suggesting that it is stiffer than other materials in this direction. The Young's modulus of the AAK-1 and AAM-1 was lower in the z-axis with 1.194 GPa and 1.235 GPa. This indicates that they are more susceptible to deformation when loaded in the z-axis.

It can be observed that asphaltenes, which are rigid and heavier components, contribute to a higher Young's modulus for AAA-1 and influence the interactions among aromatic structures. Hydrogen bonding and Van der Waals interactions are prevalent in bitumen. A denser distribution and favorable orientation of these components in AAA-1 can enhance these interactions, increasing the material's rigidity. Additionally, a more aligned chain orientation promotes effective stress transfer within AAA-1, further elevating Young's modulus materials and addressing contemporary challenges in engineering and sustainability.

The resultant Young's modulus, obtained by combining the individual directional moduli, provides an overall measure of the material's stiffness. The resultant Young's modulus was highest for AAA-1, followed by AAK-1 and AAM-1. This indicates that the overall stiffness of bitumen AAA-1 is greater than that of AAK-1 and AAM-1.

The mechanical properties of bitumen are essential to evaluate in civil engineering applications where they are incorporated as cohesive materials in asphalt pavements. At the molecular level, variations in chemical composition between AAA-1, AAK-1, and AAM-1 bitumen result in divergent network architectures. AAA-1 possesses a balanced and homogeneous molecular distribution relative to AAK-1 and AAM-1. This structural configuration leads to enhanced intermolecular attractive forces and constrained molecular mobility. When considering the scaling effects between the molecular and macro scales, the denser AAA-1 architecture translates to a material form that is inherently more cohesive.

In contrast, the more flexible topological structures in AAK-1 and AAM-1 generate bitumen whose behavior at the macroscopic scale is less restricted. Comprehending this scaling phenomenon enables civil engineers to predict mechanical response under traffic loading conditions. Given its dense nature and ensuing matrix cohesion, AAA-1 was anticipated to exhibit the highest Young's modulus. Conversely, the less constrained architectures of AAK-1 and AAM-1 suggest their moduli would be lower and comparable. Therefore, molecular insights can facilitate material selection by civil engineers by enabling forecasting of the key stiffness property of Young's modulus for designing of resilient asphalt pavements.

The results from MDS predicting Young's modulus of bitumens AAA-1, AAK-1, and AAM-1 are crucial for developing new bitumen-based materials. By providing a deep understanding of atomic-level interactions, these simulations enable the analysis of the mechanical properties of bitumens, which are essential for assessing their performance in applications like pavements. Researchers can optimize bitumen formulations by identifying the relationships between molecular structure and Young's modulus, adjusting chemical compositions to enhance stiffness, or creating composite materials by incorporating reinforcing additives or polymers.

Additionally, these findings shed light on emerging trends in smart materials. Bitumens designed to respond to environmental conditions, such as changing stiffness based on temperature or humidity, can significantly improve durability. Furthermore, integrating polymer microcapsules into bitumens can lead to self-healing properties, extending their lifespan. In the context of self-repairing pavements, this knowledge enhances the durability of infrastructure by providing materials that better withstand loads and impacts while reducing long-term maintenance costs. Overall, MDS paves the way for significant innovations in bitumen-based materials, addressing contemporary challenges in engineering and sustainability.

4. CONCLUSIONS

This analysis of the molecular dynamics of these bitumen AAA-1, AAK-1, and AAM-1 materials provides important information about their temperature-dependent behavior regarding the Young's modulus. Our results consistently demonstrate that the Young's modulus decreases as the temperature increases. This emphasizes the significance of temperature regulation and the understanding of the mechanical properties of these substances. Our research outcomes provide a precious resource for improving and establishing materials that rely heavily on temperature to influence their mechanical properties and lifespan. Future studies can broaden the temperature range and introduce nanoclusters to investigate other factors affecting Young’s modulus, such as pressure and strain rate. This will enable us to obtain a more extensive understanding of the underlying principles that operate.

REFERENCES

[1] Li, C., Liu, Q., Lei, J., Zhang, Z., Fu, C., Pan, F. (2022). Influence of mineral fillers properties on the bonding properties of bitumen mastics. Construction and Building Materials, 318: 126013. https://doi.org/10.1016/j.conbuildmat.2021.126013

[2] Nandal, M., Sood, H., Gupta, P.K. (2023). A review study on sustainable utilisation of waste in bituminous layers of flexible pavement. Case Studies in Construction Materials, 19: e02525. https://doi.org/10.1016/j.cscm.2023.e02525

[3] Mahan, H.M., Ajam, H.K.K., Jassim, H.S.H. (2023). Enhancing Marshall properties through the integration of waste plastic water bottles in dry process asphalt production. Mathematical Modelling of Engineering Problems, 10(5): 1817-1823. https://doi.org/10.18280/mmep.100534

[4] Malinowski, S., Woszuk, A., Franus, W. (2023). Modern two-component modifiers inhibiting the aging process of road bitumen. Construction and Building Materials, 409: 133838. https://doi.org/10.1016/j.conbuildmat.2023.133838

[5] Karahancer, S., Enieb, M., Saltan, M., Terzi, S., Eriskin, E., Cengizhan, A., Akbas, M.Y. (2020). Evaluating mechanical properties of bitumen and hot mix asphalt modified with nano ferric oxide. Construction and Building Materials, 234: 117381. https://doi.org/10.1016/j.conbuildmat.2019.117381

[6] Eisa, M.S., Mohamady, A., Basiouny, M.E., Abdulhamid, A., Kim, J.R. (2022). Mechanical properties of asphalt concrete modified with carbon nanotubes (CNTs). Case Studies in Construction Materials, 16: e00930. https://doi.org/10.1016/j.cscm.2022.e00930

[7] Kim, M.J., Kim, S., Yoo, D.Y., Shin, H.O. (2018). Enhancing mechanical properties of asphalt concrete using synthetic fibers. Construction and Building Materials, 178: 233-243. https://doi.org/10.1016/j.conbuildmat.2018.05.070

[8] Wei, C.J., Poovaneshvaran, S., Hasan, M.R.M., Hamzah, M.O., Valentin, J., Sani, A. (2020). Microscopic analysis and mechanical properties of Recycled Paper Mill Sludge modified asphalt mixture using granite and limestone aggregates. Construction and Building Materials, 243: 118172. https://doi.org/10.1016/j.conbuildmat.2020.118172

[9] Yao, H., Liu, J., Xu, M., Ji, J., Dai, Q., You, Z. (2022). Discussion on molecular dynamics (MD) simulations of the asphalt materials. Advances in Colloid and Interface Science, 299: 102565. https://doi.org/10.1016/j.cis.2021.102565

[10] Li, G., Chen, Z., Tan, Y., Cong, X., Dong, Y., Xiao, S. (2023). Experimental and molecular dynamics simulation of hard asphalt microstructure. Construction and Building Materials, 377: 131025. https://doi.org/10.1016/j.conbuildmat.2023.131025

[11] Tian, W., Gao, Y., Li, Y., Zhu, J., Zhan, M., Wang, S. (2023). Molecular dynamics study on the effect of rheological performance of asphalt with different plasticizers. Construction and Building Materials, 400: 132791. https://doi.org/10.1016/j.conbuildmat.2023.132791

[12] Chen, Z., Pei, J., Li, R., Xiao, F. (2018). Performance characteristics of asphalt materials based on molecular dynamics simulation - A review. Construction and Building Materials, 189: 695-710. https://doi.org/10.1016/j.conbuildmat.2018.09.038

[13] Fan, Z., Pan, F., Sun, L., Wang, D., Liu, P. (2023).

Multiscale investigation on bitumen-aggregate interfacial debonding using molecular dynamics and finite element method. Construction and Building Materials, 397: 132326. https://doi.org/10.1016/j.conbuildmat.2023.132326
[14] Luo, L., Liu, P., Oeser, M. (2022). A molecular dynamics simulation study on enhancement of thermal conductivity of bitumen by introduction of carbon nanotubes. Construction and Building Materials, 353: 129166. https://doi.org/10.1016/j.conbuildmat.2022.129166
[15] Du, J., Jin, Y., Hou, S., Jin, R., Wang, Q. (2023). Effect of component characteristics on mechanical properties of asphalt: A molecular dynamics study. Case Studies in Construction Materials, 18: e02007. https://doi.org/10.1016/j.cscm.2023.e02007
[16] Zhang, T., Gao, S., Yu, J., He, Y., Han, X., Zhuang, R. (2023). Preparation and performance of self-healing SBS modified bitumen based on dynamic disulfide bonds. Construction and Building Materials, 397: 132394. https://doi.org/10.1016/j.conbuildmat.2023.132394
[17] Chailleux, E., Queffélec, C., Borghol, I., Farcas, F., Marceau, S., Bujoli, B. (2021). Bitumen fractionation: Contribution of the individual fractions to the mechanical behavior of road binders. Construction and building materials, 271: 121528. https://doi.org/10.1016/j.conbuildmat.2020.121528
[18] Li, R., Guo, Q., Du, H., Pei, J. (2017). Mechanical property and analysis of asphalt components based on molecular dynamics simulation. Journal of Chemistry, 2017(1): 1531632. https://doi.org/10.1155/2017/1531632
[19] Li, G., Tan, Y., Fu, Y., Liu, P., Fu, C., Oeser, M. (2022). Density, zero shear viscosity and microstructure analysis of asphalt binder using molecular dynamics simulation. Construction and Building Materials, 345: 128332. https://doi.org/10.1016/j.conbuildmat.2022.128332
[20] Kang, Y., Zhou, D., Wu, Q., Liang, R., Shangguan, S., Liao, Z., Wei, N. (2019). Molecular dynamics study on the glass forming process of asphalt. Construction and Building materials, 214: 430-440. https://doi.org/10.1016/j.conbuildmat.2019.04.138
[21] Liu, Q., Fang, R., Cha, W., Wu, J., Liu, P. (2023). Influence of SARA fractions on the bitumen property using molecular dynamics simulation. https://doi.org/10.2139/ssrn.4387385
[22] Thompson, A.P., Aktulga, H.M., Berger, R., Bolintineanu, D.S., Brown, W.M., Crozier, P.S., Plimpton, S.J. (2022). LAMMPS-a flexible simulation tool for particle-based materials modeling at the atomic, meso, and continuum scales. Computer Physics Communications, 271: 108171. https://doi.org/10.1016/j.cpc.2021.108171
[23] Hou, Y., Zhang, H., Wu, J., Wang, L., Xiong, H. (2018). Study on the microscopic friction between tire and asphalt pavement based on molecular dynamics simulation. International Journal of Pavement Research and Technology, 11(2): 205-212. https://doi.org/10.1016/j.ijprt.2017.09.001
[24] Sun, H. (1994). Force field for computation of conformational energies, structures, and vibrational frequencies of aromatic polyesters. Journal of Computational Chemistry, 15(7): 752-768. https://doi.org/10.1002/jcc.540150708
[25] Sun, H. (1995). Ab initio calculations and force field development for computer simulation of polysilanes. Macromolecules, 28(3): 701-712. https://doi.org/10.1021/ma00107a006
[26] Sun, H., Mumby, S.J., Maple, J.R., Hagler, A.T. (1994). An ab initio CFF93 all-atom force field for polycarbonates. Journal of the American Chemical Society, 116(7): 2978-2987. https://doi.org/10.1021/ja00086a030
[27] Gao, Y., Zhang, Y., Zhang, C., Liu, X., Jing, R. (2022). Quantifying oxygen diffusion in bitumen films using molecular dynamics simulations. Construction and Building Materials, 331: 127325. https://doi.org/10.1016/j.conbuildmat.2022.127325
[28] Du, Z., Zhu, X., Li, F., Zhou, S., Dai, Z. (2021). Failure of the asphalt–aggregate interface under tensile stress: insight from molecular dynamics. Journal of Materials in Civil Engineering, 33(3): 04021008. https://doi.org/10.1061/(ASCE)MT.1943-5533.0003601
[29] Girgis, M., Barbier, J., Quignard, A., Merdrignac, I., Marques, J. (2021). Correlation and modelling of the penetration and softening point tests of bitumen binders with a variety of physical and chemical properties. Oil & Gas Science and Technology–Revue d'IFP Energies nouvelles, 76：57. https://doi.org/10.2516/ogst/2021046
[30] Laux, D., Toulgoat, K., Millot, L., Ferrandis, J.Y. (2024). Rheological investigation of bitumen, used for radioactive waste conditioning, with ultrasonic waves. EPJ N-Nuclear Sciences & Technologies, 10: 1. https://doi.org/10.1051/epjn/2024002
[31] Lesueur, D. (2009). The colloidal structure of bitumen: Consequences on the rheology and on the mechanisms of bitumen modification. Journal Advances in Colloid and Interface Science, 145: 42-82. https://doi.org/10.1016/j.cis.2008.08.011
[32] Li, D.D., Greenfield, M.L. (2014). Chemical compositions of improved model asphalt systems for molecular simulations. Fuel, 115: 347-356. https://doi.org/10.1016/j.fuel.2013.07.012
[33] Belabdelouahab, F., Trouzine, H., Hellal, H., Rahali, B., Ould Kaci, S., Medine, M. (2018). Comparative analysis of estimated young's modulus of rubberized mortar and concrete. International Journal of Civil Engineering, 16: 243-253. https://doi.org/10.1007/s40999-016-0119-x
[34] Robertson, R.E., Branthaver, J.F., Harnsberger, P.M., Petersen, J.C., Dorrence, S.M., McKay, J.F., Turner, T.F., Pauli, A.T., Huang, S.C., Huh, J.D., Tauer, J., Thomas, K.P., Netzel, D.A., Miknis, F.P., Williams, T.M., Duvall, J.J., Barbour, F.A., Wright, C. (2001), Fundamental Properties of Asphalts and Modified Asphalts. Interpretive Report (No. FHWA-RD-99-212), United States. Federal Highway Administration.
[35] Sun, W., Wang, H. (2020). Moisture effect on nanostructure and adhesion energy of asphalt on aggregate surface: A molecular dynamics study. Applied Surface Science, 510: 145435. https://doi.org/10.1016/j.apsusc.2020.145435
[36] Xu, G., Wang, H. (2016). Molecular dynamics study of interfacial mechanical behavior between asphalt binder and mineral aggregate. Construction and Building Materials, 121: 246-254. https://doi.org/10.1016/j.conbuildmat.2016.05.167
[37] Zhang, L., Greenfield, M.L. (2008). Effects of polymer modification on properties and microstructure of model

asphalt systems. Energy & Fuels, 22(5): 3363-3375. https://doi.org/10.1021/ef700699p
[38] Luo, Y., Teng, G. (2021). Self-healing performance of rubber-modified asphalt. Environmental & Earth Sciences Research Journal, 8(2): 75-80. https://doi.org/10.18280/eesrj.080202
[39] Xu, W., Qiu, X., Xiao, S., Hu, G., Wang, F., Yuan, J. (2020). Molecular dynamic investigations on the adhesion behaviors of asphalt mastic–aggregate interface. Materials, 13(22): 5061. https://doi.org/10.3390/ma13225061
[40] Xu, G., Wang, H. (2016). Study of cohesion and adhesion properties of asphalt concrete with molecular dynamics simulation. Computational Materials Science, 112: 161-169. https://doi.org/10.1016/j.commatsci.2015.10.024
[41] Sun, G., Niu, Z., Zhang, J., Tan, X., Jing, Y., Chen, Z. (2022). Impacts of asphalt and mineral types on interfacial behaviors: A molecular dynamics study. Case Studies in Construction Materials, 17: e01581. https://doi.org/10.1016/j.cscm.2022.e01581
[42] Harrison, I.R., Wang, G., Hsu, T.C. (1992). A differential scanning calorimetry study of asphalt binders. The National Academies of Sciences, Engineering, and Medicine. https://doi.org/10.3390/buildings13071608
[43] Jiao, Y., Yao, Y., Qiu, H., Chen, H., Wu, Y. (2024). A molecular dynamics analysis of the thickness and adhesion characteristics of the quasi-liquid layer at the asphalt–ice interface. Materials, 17(6): 1375. https://doi.org/10.3390/ma17061375
[44] Fallah, F., Khabaz, F., Kim, Y.R., Kommidi, S.R., Haghshenas, H.F. (2019). Molecular dynamics modeling and simulation of bituminous binder chemical aging due to variation of oxidation level and saturate-aromatic-resin -asphaltene fraction. Fuel, 237: 71-80. https://doi.org/10.1016/j.fuel.2018.09.110
[45] Hamedi, G.H., Shabani, A., Safargar, Y. (2020). Investigating the effect of hydrophobic additives in moisture damage reduction of asphalt mixtures. Periodica Polytechnica Civil Engineering, 64(3): 702-712. https://doi.org/10.3311/PPci.15457
[46] Durmaz, C., Sengoz, B., Ozdemir, D.K., Topal, A. (2021). Investigation of different laboratory aging methods of bituminous mixtures. Periodica Polytechnica Civil Engineering, 65(2): 537-545. https://doi.org/10.3311/PPci.15480
[47] Rosta, S., Gaspar, L. (2023). Dynamic viscosity prediction of blends of paving grade bitumen with reclaimed bitumen. Periodica Polytechnica Transportation Engineering, 51(3): 263-269. https://doi.org/10.3311/PPtr.21926
[48] Ramdan, K.Z., Abo-Qudais, S.A. (2017). Effect of superpave short-term aging on binder and asphalt mixture rheology. Periodica Polytechnica Transportation Engineering, 45(4): 196-205. https://doi.org/10.3311/PPtr.10477
[49] Yao, H., Dai, Q., You, Z., Bick, A., Wang, M. (2018). Modulus simulation of asphalt binder models using Molecular Dynamics (MD) method. Construction and Building Materials, 162: 430-441. https://doi.org/10.1016/j.conbuildmat.2017.09.106
[50] Dourado, E.R., Simao, R.A., Leite, L.F.M. (2012). Mechanical properties of asphalt binders evaluated by atomic force microscopy. Journal of Microscopy, 245: 119-128. https://doi.org/10.1111/j.1365-2818.2011.03552.x
[51] Huang, G., Zhang, J., Hui, B., Zhang, H., Guan, Y., Guo, F., Li, Y., He, Y., Wang, D. (2023). Analysis of modulus properties of high-modulus asphalt mixture and its new evaluation index of rutting resistance. Sustainability, 15(9): 7574. https://doi.org/10.3390/su15097574
[52] Zhuang, S., Wang, J., Li, M., Yang, C., Chen, J., Zhang, X., Zhao, Z., Li, D., Ren, J. (2023). Rutting and fatigue resistance of high-modulus asphalt mixture considering the combined effects of moisture content and temperature. Buildings, 13(7): 1608. https://doi.org/10.3390/buildings13071608